Chemistry & Biology 13, 549–556, May 2006 DOI 10.1016/j.chembiol.2005.12.009

Antagonists to Human and Mouse Vascular Endothelial Growth Factor Receptor 2 Generated by Directed Protein Evolution In Vitro

Elena V. Getmanova,[1,2,3] Yan Chen,[1,2,4] Laird Bloom,[1,5] Jochem Gokemeijer,[1,6] Steven Shamah,[1,7] Veena Warikoo,[1,8] Jack Wang,[1,6] Vincent Ling,[6] and Lin Sun[1,3,*]

[1] Phylos, Inc., succeeded by Compound Therapeutics, Inc.
100 Beaver Street
Waltham, Massachusetts 02453

Summary

Using directed in vitro protein evolution, we generated proteins that bound and antagonized the function of vascular endothelial growth factor receptor 2 (VEGFR2). Binders to human VEGFR2 (KDR) with 10–200 nM affinities were selected by using mRNA display from a library (10^{13} variants) based on the tenth human fibronectin type III domain (10Fn3) scaffold. Subsequently, a single KDR binding clone (K_d = 11 nM) was subjected to affinity maturation. This yielded improved KDR binding molecules with affinities ranging from 0.06 to 2 nM. Molecules with dual binding specificities (human/mouse) were also isolated by using both KDR and Flk-1 (mouse VEGFR2) as targets in selection. Proteins encoded by the selected clones bound VEGFR2-expressing cells and inhibited their VEGF-dependent proliferation. Our results demonstrate the potential of these inhibitors in the development of anti-angiogenesis therapeutics.

Introduction

Directed protein evolution has shown promise in harnessing desired changes in the properties and functionalities of proteins. Several techniques that couple proteins to their coding information have made it possible to carry out directed protein evolution by in vitro selection [1–3], and this allows for the rapid identification of desired molecules from libraries with large numbers of variants. Folded polypeptide frameworks provide useful scaffolds for presenting amino acid variability in a protein library [4]. From a therapeutic perspective, the optimal binding protein should be of human origin to minimize immunogenicity, it should be sufficiently stable to be expressed in a microbial system at high levels, and it should be adaptable so as to accommodate the changes needed to allow specific target binding and biological functionality. The tenth human fibronectin type III domain (10Fn3), a stable, small protein (10 kD, Tm > 80ºC) with a folded structure similar to the variable domains of antibodies, has been exploited to develop binding molecules to a diverse array of targets [5–8]. However, to date, no biological activities have been reported for any binding molecule derived from this scaffold.

In this study, we exploited the 10Fn3 scaffold to target vascular endothelial growth factor receptor 2 (VEGFR2). VEGF and two of its receptors, VEGFR1 (*fms*-like tyrosine kinase1, Flt-1) and VEGFR2 (kinase insert domain receptor, KDR), are major regulators of endothelial cell activities, including vasculogenesis and angiogenesis [9]. Angiogenesis, the formation of new blood vessels from preexisting vasculature, occurs under both normal and pathologic conditions. VEGFR2 activation plays a major role in pathological angiogenesis [10] and has been targeted for cancer therapeutic intervention. A number of inhibitors of angiogenesis have been identified, including naturally occurring factors such as angiostatin and endostatin [11], engineered natural biologics such as VEGF-trap [12], and synthetic small molecules, peptides, oligonucleotides, and antibodies [13]. Many such inhibitors have shown promising neutralizing activities in biological assays and animal model studies, and some have demonstrated medical benefit in controlled clinical studies. For example, the anti-VEGF antibody Avastin (Bevacizumab) [14] has been shown to be beneficial to patients suffering from late stages of colon, non-small-cell lung, and breast cancers. Here, we report the first example of engineered biological inhibitors to VEGFR2 discovered by altering a natural human protein domain through molecular evolution by mRNA display, an in vitro display technology that allows a covalent linkage of a protein and its coding mRNA [15, 16]. The identification of this new class of binding molecules demonstrates the potential of this engineered scaffold in generating novel therapeutic proteins.

Results and Discussion

Initial Identification of KDR Binding Molecules

A 10Fn3 mRNA fusion library (10^{13} variants) was used in in vitro selection against the extracellular domain of human VEGFR2. After 6 rounds of selection, 30 independent clones were tested for binding to KDR, and the best binders were subsequently tested for binding in the presence of VEGF (Figure 1A). VEGF inhibited target binding of multiple clones, suggesting that these binders may interfere with the natural VEGF-KDR interaction. Indeed, in a BIAcore assay, binders VR28 and VR12, but not a noncompeting clone (VR17), inhibited KDR binding to immobilized VEGF in a dose-dependent manner (Figure 1B). VR28 protein also bound KDR-expressing recombinant CHO cells, but not control CHO cells (Figure 1C). VR28 had the best affinity to KDR

*Correspondence: lsun@ccib.mgh.harvard.edu
[2] These authors contributed equally to this work.
[3] Present address: Center for Computational and Integrative Biology, Massachusetts General Hospital, 38 Sidney Street, Suite 100, Cambridge, Massachusetts 02139.
[4] Present address: Novartis Institutes for BioMedical Research, Inc., Cambridge, Massachusetts 02139.
[5] Present address: Wyeth Pharmaceuticals, Cambridge, Massachusetts 02140.
[6] Present address: Compound Therapeutics, Inc., Waltham, Massachusetts 02453.
[7] Present address: Archemix Corporation, Cambridge, Massachusetts 02139.
[8] Present address: GTC Biotherapeutics, Inc., Framingham, Massachusetts 01702.

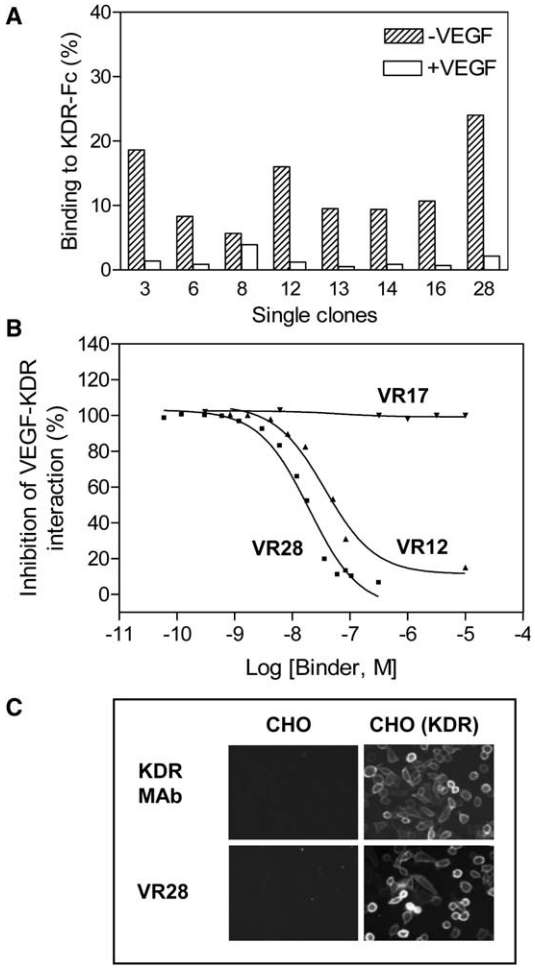

Figure 1. Characterization of Clones Isolated from Initial KDR Selection

(A) VEGF inhibits interaction between KDR and selected binding molecules. A radioactive equilibrium binding assay was performed with clones from Round 6 (0.1 pmol) with KDR-Fc (2.5 pmol) in the presence or absence of VEGF (10 pmol). Binding was expressed as a percentage of input binder material. Nonspecific binding to the beads in the absence of KDR-Fc represented less than 2%.

(B) Recombinant binder proteins disrupt the VEGF and KDR interaction. Binding of KDR-Fc (2.5 pmol) to immobilized VEGF (2.5 pmol) in the presence of different concentrations of VR28, VR12, and VR17 was evaluated in a BIAcore binding assay. RU detected by KDR-Fc binding in the absence of competitor was assigned as 100%.

(C) VR28 binding to KDR-expressing CHO (KDR) and control CHO cells was detected by an immunofluorescent sandwich assay by using fluorescent microscopy.

(11–13 nM) among the tested clones, but it showed little inhibition of VEGF-KDR signaling in a VEGF-dependent cell proliferation assay (IC_{50} > 200 nM, data not shown). Thus, while the initial selection from the naïve library yielded multiple binding molecules that interfered with the interaction between VEGF and KDR in biochemical binding studies, affinity improvements appeared to be necessary for neutralizing KDR function in a biological assay, perhaps due to the high-affinity interaction between VEGF and KDR (75–125 pM) [17]. VR28 was chosen for affinity maturation since it had the best binding affinity to KDR, had the ability to inhibit VEGF and KDR interaction in binding studies in vitro, and lacked mutations in the framework regions.

Affinity Maturation of the VR28 Clone

The sequence of the binding loops of VR28 is shown in Table 1. We initially constructed libraries by introducing mutations to all three loops of VR28 by using hypermutagenic PCR. Selection against KDR from these libraries yielded binding molecules with moderate affinity improvement (a K_d as low as 1 nM, data not shown). Although many beneficial mutations were selected in the FG loop (for example, V77M, Q79R, N80S, D81G, H82R, and I85F), mutations in the BC and DE loops appeared to be random and didn't further improve affinity to KDR. Furthermore, reverse selection to VR28 BC and DE loop amino acids was evident, as indicated by different codon usages in selected clones. Overall, despite a similar average mutation rate of the three loop regions prior to selection (BC = 28.6%, DE = 31.6%, FG = 22.3%), the FG loop of selected clones (n = 100) revealed approximately 5-fold more mutations than the BC and DE loops (19.3%, 3.5%, and 4.2%, respectively), suggesting a greater potential to target the FG loop sequence for additional affinity improvements.

Two incidental mutations in the N-terminal region, L8P and L8Q, also resulted in better binding to KDR in a number of selected clones. Several residues in the N terminus of the 10Fn3 domain are located in close proximity to the FG loop based on structure studies [18]. This could potentially have a negative impact on target binding. A location change of the N terminus relative to the FG loop, perhaps as a result of Leu8 mutations, could presumably improve KDR binding affinity. Indeed, deletion of the first eight amino acids from the N terminus of these clones improved binding to KDR (data not shown).

Consequently, new libraries (with or without the N-terminal deletion) were constructed to introduce mutations

Table 1. VEGFR2 Binding Clones

Clone	BC Loop (23–29)	DE Loop (52–55)	FG Loop (77–86), P87
WT	DAPAVTV	GSKS	GRGDSPASSKP
VR28	RHPHFPT	LQPP	VAQNDHELITP
K1	RHPHFPT	LQPP	**MGLYG**HELLTP
K6	RHPHFPT	LQPP	**DGKDGRVLL**TP
K9	RHPHFPT	LQPP	**FGLYGKELLI**P
K10	RHPHFPT	LQPP	**TGPNDRLLFV**P
K12	RHPHFPT	LQPP	**DVYNDHEIKT**P
K13	RHPHFPT	LQPP	**LALKGHELLT**P
K14	RHPHFPT	LQPP	**REE**NDHELLIP
K15	RHPHFPT	LQPP	**EVHHDREIKT**P
E3	RHPHFPT	LQPP	**DGRNDRKLMV**P
E5	RHPHFPT	LQPP	**DGQNGRLLNV**P
E6	RHPHFPT	LQPP	**DGWNGRLLSI**P
E9	RHPHFPT	LQPP	**EERNGRTLRT**P
E18	RHPHFPT	LQPP	**VERNGRELNT**P
E19	RHPHFPT	LQPP	**VERNGRHLMT**P
E25	RHPHFPT	LQPP	**LERNGRELMT**P
E26	RHPHFPT	LQPP	**VERNGRELMT**P
E28	RHPHFPT	LQPP	**LERNGRELMV**P
E29	RHPHFPT	LQPP	**VERNGRVLMT**P

The FG loop residues in bold indicate residues different from the parental clone VR28.

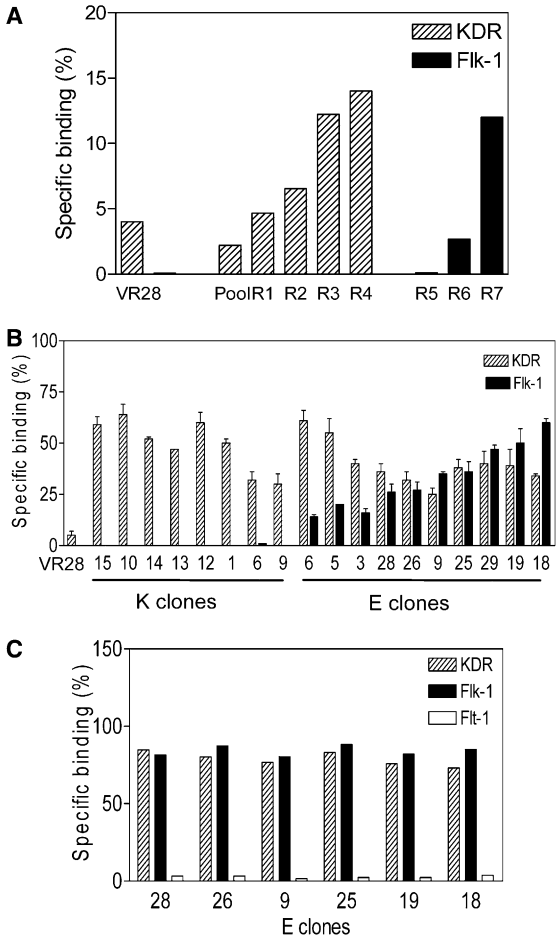

Figure 2. Affinity Maturation of VR28

Binding was measured in a radioactive equilibrium assay.

(A) VR28, starting pool, and selected populations to 1 nM KDR-Fc or Flk-1-Fc.

(B) Clones from Round 4 (K clones) and Round 7 (E clones) to 1 nM KDR-Fc and Flk-1-Fc. The data represent an average of three independent experiments.

(C) Clones from Round 7 (E clones) to 100 nM KDR-Fc, Flk-1-Fc, or Flt-1-Fc.

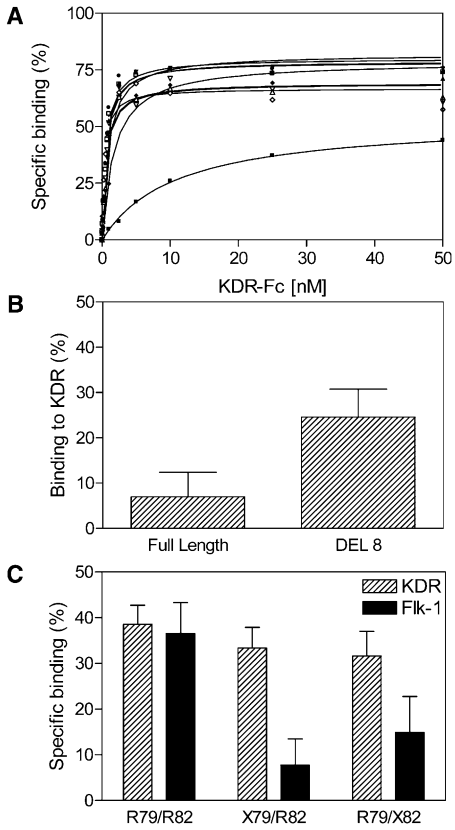

Figure 3. Affinity Maturation Yielded KDR Binding Proteins with Improved Binding Affinity

(A) Binding affinities to KDR as measured in a radioactive equilibrium binding assay for VR28 (■; K_d = 11 ± 0.5 nM) and selected clones from Round 4: K1 (▲; K_d = 0.6 ± 0.1), K6 (▼; K_d = 0.9 ± 0.1), K9 (◆; K_d = 1.8 ± 0.4), K10 (●; K_d = 0.6 ± 0.1), K12 (□; K_d = 0.6 ± 0.1), K13 (△; K_d = 0.6 ± 0.1), K14 (▽; K_d = 0.6 ± 0.1), and K15 (◇; K_d = 0.4 ± 0.1).

(B) N terminus deletion improved binding to KDR. The data represent an average binding to 1 nM KDR of 23 independent clones with and without deletion of the first 8 amino acid residues in the N terminus.

(C) Two arginine residues are important for binding to Flk-1. When the arginine at position 79 or position 82 was replaced by other amino acids (X79 = E, Q, W, P; X82 = L, K), binding to Flk-1, but not to KDR, decreased significantly. Clones from Round 7 of affinity maturation selection were analyzed for binding to 1 nM KDR and Flk-1 in a radioactive equilibrium binding assay. The data represent an average binding of four (R79), seven (X79), three (R82), and four (X82) independent clones from Round 7.

to the FG loop of VR28 by using oligonucleotide-derived mutagenesis, which resulted in more than six amino acid changes per FG loop. Lower KDR concentrations were utilized during selection to favor clones with better affinities. The N-terminal deletion yielded higher KDR binding activity than the nondeleted population. Target binding of selection populations and clones from Round 4 is shown in Figure 2. The affinity binding constants of individual clones to KDR ranged from 0.32 to 1.8 nM, a 10- to 30-fold improvement over VR28 (11 nM) (Figure 3A). The binding activity appeared to be specific to KDR rather than to the Fc portion since several tested clones didn't bind to high concentrations of IgG-Fc (data not shown); this finding indicated that the negative selection (preclear) against IgG was effective in suppressing Fc binders.

Sequence analysis of the selected clones from affinity maturation through oligo-based mutagenesis revealed that while the binding population was diverse, several consensus motifs were present (Table 1, K clones). Most noticeably, as in VR28, Pro87 and Leu84 were found in nearly all clones, suggesting that these residues may be essential for the binding site. A positively charged amino acid at position 82 appears to be required, since only H82K or H82R changes were seen in the sequenced clones. Aliphatic amino acid was predominant at position 78. D81 was often mutated to a G, resulting in the loss of negative charge at this position and a potential gain in flexibility. The overall mutation rate in the selected population was comparable to the pool prior to selection, suggesting that the FG loop is very tolerant to structural changes. To further verify the impact of the N terminus on target binding, we created variants with and without the N terminus deletion of 23 clones from Round 4. Binding to KDR was

improved for all but one clone with the deletion; this lone clone showed no change in binding. On average, the deletion resulted in an ~3-fold improvement in binding (Figure 3B).

Selection of Binders with Dual Specificities to Human and Mouse VEGFR2

VR28 and most of the affinity-matured variants (K clones) failed to bind Flk-1, as shown in Figure 2B. However, since KDR and Flk-1 share a high level (85%) of sequence identity, and since both can be activated by human VEGF [19, 20], it is conceivable that novel variants can be evolved to bind both KDR and Flk-1, presumably by recognizing similar residues or structures shared by KDR and Flk-1. This will allow the same molecule to be tested in functional studies in animal models and, subsequently, in humans.

Therefore, the population that had been selected for four rounds against KDR was further selected against Flk-1. As shown in Figure 2, an increase in binding to Flk-1 was observed from Round 5 to Round 7, indicating enrichment of Flk-1 binders. In contrast to the clones selected against KDR only (K clones), most clones derived from additional selection against Flk-1 (E clones) are able to interact with both KDR and Flk-1 (Figure 2B). The binding analysis, shown in Table 2, indicates that the clones were able to bind both targets with high affinities. For example, E19 has a K_d of 56 pM to KDR and a K_d of 340 pM to Flk-1. The target switch strategy has allowed for the isolation of molecules with dual binding specificities to both KDR and Flk-1 from a mutagenized population of VR28, a moderate KDR binder that was not able to bind Flk-1. The selected binders are highly specific to VEGFR2, as no substantial binding to VEGFR1, which shares 31% sequence identity to VEGFR2 in its extracellular domain [21], was observed at a high target concentration (Figure 2C). Specific binding to KDR would be desirable for a therapeutic candidate to reduce the risk of side effects.

Sequence analysis (Table 1) revealed some motifs similar to those observed in the KDR binder pool (Leu and Pro at residues 84 and 87, respectively; positively charged amino acid at residue 82 [predominantly Arg]) and some that were not maintained (aliphatic at position 78). In addition, while the motif ERNGR (residues 78–82) was present in almost all clones binding to Flk-1, it was rarely found in the populations selected on KDR only. R79 and R82 appear to be particularly important for high-affinity binding to Flk-1, since binding to Flk-1, but not KDR, is greatly reduced when a different residue is present at this position (Figure 3C).

To determine whether all three loops are required for target binding, the loop sequences of clones E6 and E26 were substituted one at a time by a randomized sequence of corresponding length encoded by NNS. The resulting populations were expressed by in vitro translation and were purified by a C-terminal FLAG tag. Therefore, the purified proteins should be devoid of sequences containing frameshifts and stop codons. Proteins derived from each loop replacement failed to bind the target (data not shown). This result suggests that any combination of just two nonrandomized loops may not be sufficient for target binding. A second possibility is that a large portion of the randomized loop sequences was incompatible with the rest of the domain, resulting in unfolded proteins. In the context of VR28, point mutations of P25 or F27 in the BC loop and L52, Q53, or P54 in the DE loop eliminated binding to KDR (data not shown). In addition, when a loop of another KDR binder was replaced by the analogous wild-type 10Fn3 loop, target binding was abolished [22]. Together, these results suggest that the selected loop sequences are involved in binding in a coordinated fashion, and that each one plays a role in interacting with the target and/or in maintaining the properly folded structure of the protein. The requirement of all three loops also suggests that the randomization strategy allowed 10Fn3 to maintain a folded structure for proper display of varied sequences in the three loop segments.

Table 2. Affinity of Selected Binders

Clone	Target	In Vitro K_d (nM)	K_a (1/M*s) × 10^5	K_d (1/s) × 10^{-5}	BIAcore K_d (nM)
E6	KDR	0.4 ± 0.1	8.9	6.7	0.08
	Flk-1	7.1 ± 1.1	6.7	136.0	2.02
E18	KDR	1.2 ± 0.2	2.6	12.1	0.46
	Flk-1	0.5 ± 0.1	6.0	19.5	0.33
E19	KDR	1.3 ± 0.2	3.0	1.7	0.06
	Flk-1	0.7 ± 0.1	6.6	22.3	0.34
E25	KDR	1.6 ± 0.4	2.5	5.2	0.21
	Flk-1	1.3 ± 0.2	5.0	37.8	0.76
E26	KDR	1.7 ± 0.4	1.1	5.8	0.51
	Flk-1	2.0 ± 0.3	2.2	47.7	2.14
E29	KDR	1.5 ± 0.4	3.6	7.0	0.19
	Flk-1	0.9 ± 0.2	7.9	28.8	0.37

Selected Binders Interact with Cell Surface-Expressed VEGFR2 and Neutralize Its Function

The ultimate therapeutic utility of the selected KDR binding molecules will depend heavily on their functionality after recombinant production. We expressed a number of the binding molecules in an *E. coli* expression system and purified them from soluble fraction by affinity chromatography via a His_6 tag. The expression level and solubility varied between binders; however, in many cases, we were able to purify 20–40 mg protein/l culture from the soluble fraction. The stability of the binders derived from 10Fn3 differed from binder to binder [22], and Tm values ranged from 37ºC to 65ºC (data not shown).

Using a detection system consisting of a primary mouse anti-His_6 tag antibody followed by a fluorescently labeled secondary antibody, the recombinant binding molecules were shown to bind specifically to mammalian cells expressing KDR or Flk-1 with low nanomolar IC_{50}, while no binding was observed for wild-type 10Fn3 (Figure 4). Furthermore, many selected clones inhibited VEGF-stimulated cell proliferation in a dose-dependent fashion, with IC_{50}s as low as 3–12 nM for KDR-expressing cells and 2–5 nM for Flk-1-expressing cells. The potency of inhibition appeared to be similar to that of the control anti-KDR and anti-Flk-1 monoclonal antibodies, as shown in Figure 5.

A number of clones were further tested for inhibitory activity against HUVEC cells that require VEGF for proliferation. As shown in Figure 5C, the KDR binding molecules were also active in antagonizing VEGF activity in this human cell system; though, the wild-type 10Fn3

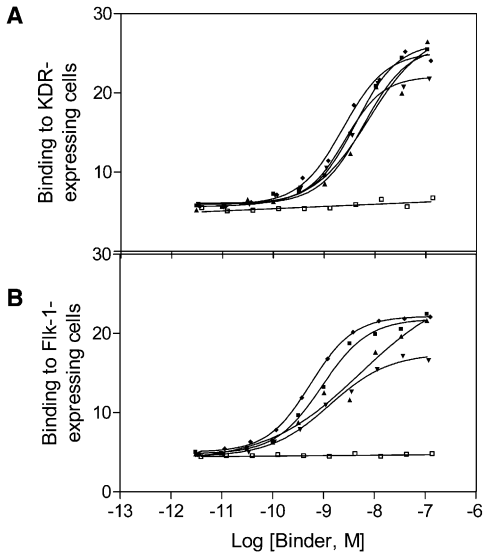

Figure 4. Affinity-Matured Proteins Specifically Bind to VEGFR2-Expressing Cells

(A) Binding of E18 (■; IC_{50} = 4.2 ± 1.0), E19 (▲; IC_{50} = 7.6 ± 1.7), E26 (▼; IC_{50} = 2.6 ± 1.2), E29 (◆; IC_{50} = 2.3 ± 1.0), and WT (□; n.d.) to CHO-KDR cells expressing human KDR.

(B) Binding of E18 (■; IC_{50} = 0.9 ± 0.4), E19 (▲; IC_{50} = 5.3 ± 2.5), E26 (▼; IC_{50} = 1.3 ± 0.7), E29 (◆; IC_{50} = 0.6 ± 0.1), and WT (□; n.d.) to CHO-Flk-1 cells expressing Epo-Flk-1 chimera. No binding was detected to control CHO cells (data not shown).

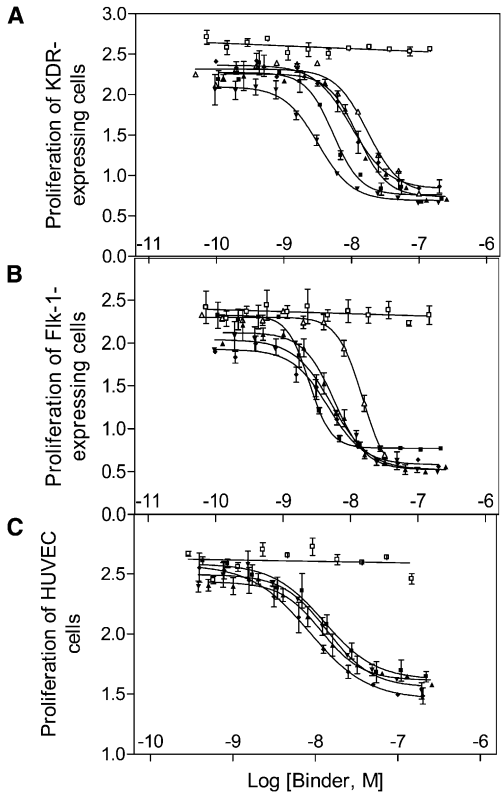

Figure 5. Affinity-Matured Binding Proteins Antagonize VEGFR2 Function

(A–C) *E. coli*-produced VEGFR2 binding proteins and control anti-VEGFR2 antibodies were tested for inhibition to VEGF-dependent cell proliferation as measured by absorbance at 490 nm using Cell Titer 96. (A) KDR-expressing cells (Ba/F3-KDR): E18 (■; IC_{50} = 5.4 ± 1.2 nM), E19 (▲; IC_{50} = 12.3 ± 2.6), E26 (▼; IC_{50} = 3.2 ± 0.5), E29 (◆; IC_{50} = 10.0 ± 2.1), WT (□; n.d.), and anti-KDR antibody (△; IC_{50} = 17.3 ± 7.7); (B) Flk-1-expressing cells (Ba/F3-Flk-1): E18 (■; IC_{50} = 2.4 ± 0.2), E19 (▲; IC_{50} = 5.8 ± 1.0), E26 (▼; IC_{50} = 5.3 ± 1.7), E29 (◆; IC_{50} = 4.7 ± 1.2), WT (□; n.d.), and anti-Flk-1 antibody (△; IC_{50} = 15.0 ± 3.2); and (C) human umbilical vein endothelial cells (HUVEC): E18 (■; IC_{50} = 12.8 ± 4.6), E19 (▲; IC_{50} = 11.8 ± 2.7), E26 (▼; IC_{50} = 14.0 ± 5.9), E29 (◆; IC_{50} = 8.4 ± 0.8), and WT (□; n.d.). The data represent an average of two independent experiments. No inhibition was observed for control cells (Ba/F3-TrkB) that required NT4 for proliferation (data not shown).

was inactive. The IC_{50} of these inhibitors to KDR is ~10 nM, a concentration approaching utility for biotherapeutic candidates.

The improved binding affinity of KDR binders resulted in their ability to inhibit VEGF-dependent cell proliferation with low nanomolar IC_{50}, suggesting a direct correlation between affinities and neutralizing activity. Since the binding population was diverse, it is possible that still more potent inhibitors may exist in this population; however, they were not identified due to our limited sampling size of individual clones. Additional stringent selection may allow for the identification of those clones.

Significance

Interaction between vascular endothelial growth factor (VEGF) and its receptors plays a central role in angiogenesis. Antagonists that disrupt this interaction are shown to have clinical utility in the treatment of neoplastic diseases and retinal angiopathies. We report here the identification of a class of engineered proteins capable of inhibiting VEGFR2. Using mRNA display and directed protein evolution, we sampled a library based on the tenth human fibronectin type III domain and identified molecules with nanomolar affinity to human VEGFR2. Upon affinity maturation of a progenitor clone (K_d = 11 nM), descendant binding molecules bound the target with subnanomolar affinity (as low as 60 pM) and disrupted the function of VEGFR2 in a number of cell types with a low nanomolar IC_{50} comparable to that observed for a high-affinity anti-KDR antibody [23]. These relatively small proteins (10 kD) can offer advantages in situations (such as tissue penetration and manufacturing) where larger protein therapeutics (such as antibodies) are limited. Using a novel mutagenesis and selection strategy, we identified binding molecules to both human and mouse VEGFR2 by targeted randomization of a KDR binder that originally did not bind Flk-1. This makes it possible for the same molecules to be used in studies in mouse and human subjects, allowing for the avoidance of pitfalls that may be associated with a molecule switch between these studies. Our work demonstrates for the first time that these VEGFR2 antagonists have the potential to be developed as therapeutics to inhibit pathologic angiogenesis.

Experimental Procedures

Recombinant Proteins

Human and murine VEGF, human neurotrophin-4 (NT4), and human and mouse VEGFR2 Fc (KDR-Fc and Flk-1-Fc) were purchased from R&D Systems (Minneapolis, MN).

Primary Library Construction

The construction of the library with 10Fn3 as a scaffold was previously described [6]. Three loop regions, BC, DE, and FG, corresponding to positions 23–29, 52–55, and 77–86, respectively, were randomized by using NNS as the coding scheme. This library contained $\sim 1 \times 10^{13}$ members and was used in the KDR selection that identified the initial KDR binding clones, including VR28.

Mutagenic Library Construction

Hypermutagenic PCR

An incidental scaffold mutation, T69I, in VR28 was corrected by PCR with no change in its binding activity to KDR (data not shown). Using hypermutagenic PCR (1 mM dGTP, 0.03 mM dCTP, 1 mM dTTP, 0.03 mM dATP, 0.5 mM Mn^{2+}) [24] with loop flanking primers, we introduced mutations to each of the three loops of VR28. One, two, or three rounds of PCR were conducted separately on each of the three loops. The resulting fragments from each round of mutagenesis were combined, and the libraries were assembled by using overlap extension and PCR. A total of 10–15 clones from each round of mutagenesis were analyzed by sequencing, and the mutagenesis rate was found to be similar to published results [24]. On average, each round of mutagenic PCR resulted in 10% amino acid mutations in all three loops (18% for one round, 27% for two rounds, and 33% for three rounds). We observed 1.5% framework mutations after three rounds, a value significantly lower than that of the targeted loop regions (33%). Mutagenized libraries showed significantly reduced binding to KDR: 5.6%, 1.6%, and 1.0% binding to 25 nM KDR for libraries from one, two, and three rounds, respectively, as compared to 24% for VR28 (data not shown). The three libraries were combined at equal molar ratio and were subjected to selection against 1 nM KDR.

Oligo-Based Mutagenesis

The FG loop (residues 77–86; VAQNDHELIT) and position Pro87 of VR28 were mutagenized by oligonucleotide VR28FG-50, containing 50% of the VR28 nucleotide and 50% of N or S at each position, which resulted in ~67% random amino acid changes in the FG loop and Pro87. The sequence of VR28FG-50 was 5′-gtg tat gct gtc act g/n t/n g/s g/n c/n c/s c/n a/n g/s a/n a/n c/s g/n a/n c/s c/n a/n c/s g/n a/n g/s c/n t/n c/s a/n t/n c/s a/n c/n c/s c/n c/n a/s att tcc att aat tac-3′. The mutagenized library was assembled by PCR. DNA sequencing of library members confirmed the intended mutation rate.

Mutagenesis of Flk-1 binding clones (E clones) was conducted with primers with NNS at all loop positions, resulting in fully randomized BC, DE, or FG loops. Deletion of the N-terminal eight amino acid residues was carried out by using standard PCR techniques. All constructs and mutagenic libraries contained T7 TMV promoter and Flag tag sequences at the 5′ and 3′ flanking regions, respectively, for production and purification of mRNA fusion molecules and proteins.

mRNA Fusion Production

For each round of selection, DNA from PCR was transcribed by using the MegaScript transcription kit (Ambion). The puromycin-containing linker TEG 6/10 was synthesized and crosslinked to RNA as previously described [25]. The crosslinked mixture was included in an in vitro translation reaction by using the rabbit reticulocyte lysate translation kit (Ambion) in the presence of ^{35}S-labeled methionine at 30ºC for 60 min. To enhance the fusion formation, 0.5 M KCl and 0.05 M $MgCl_2$ were added to the reaction and incubated for 30 min at 4ºC. Fusion molecules were purified by using oligo-dT cellulose chromatography. A reverse transcription reaction was conducted with SuperScript II (Invitrogen) for 1 hr at 42ºC with the primer Hu3′FLAGSTOP (5′-ttttaaatagcggatgccttgtcgtcgtcgtccttgtagtctgttcggtaattaatgg-3′). Reactive cysteine residues were modified for 1 hr at room temperature with 1 mM 2-nitro-5-thiocyanatobenzoic acid or N-ethylmaleimide at alternative rounds for the first four rounds of selection. Fusion molecules were further purified by anti-FLAG affinity chromatography by using M2 agarose (Sigma). The fusion yield was calculated based on specific activity measured by scintillation counting of ^{35}S-methionine in the samples.

Selection

Primary Selection against KDR

A fusion library ($\sim 10^{13}$ variants in 1 ml) was incubated with 100 μl Protein A beads (Dynal) prebound to human IgG for 1 hr at 30ºC prior to selection (preclear). The supernatant was then incubated in buffer A (50 mM HEPES, 150 mM NaCl, 0.02% Triton X-100, 1 mg/ml bovine serum albumin [BSA], 0.1 mg/ml salmon sperm DNA [pH 7.4]) with KDR-Fc for 1 hr at 30ºC. The target was captured on 300 μl (round 1) or 100 μl (rounds 2–6) Protein A beads for 30 min at 30ºC, and beads were washed five times with 1 ml buffer A without BSA and salmon sperm DNA. Bound fusion molecules were eluted with 100 μl 0.1 M KOH into 50 μl 1 M Tris-HCl (pH 8.0). DNA was amplified by PCR by using flanking primers. Final concentrations of KDR-Fc were 250 nM (round 1), 100 nM (rounds 2–4), and 10 nM (rounds 5 and 6).

Affinity and Specificity Maturation of KDR Binder VR28

mRNA fusion libraries of mutagenized VR28 were produced as described above. Following preclear with Protein A beads prebound to human IgG, selection was performed in buffer B (1× PBS, 0.02% Triton X-100, 1 mg/ml BSA, 0.1 mg/ml salmon sperm DNA [pH 7.4]) for five rounds at 1 nM KDR. Libraries derived from oligo-based mutagenesis were selected for four rounds at 0.1 nM KDR and three additional rounds at 1 nM mouse VEGFR2 (Flk-1). Selections were stopped when no further increase in binding to the target was observed.

Radioactive Equilibrium Binding Assay

^{35}S-labeled binder proteins were produced in a rabbit reticulocyte lysate translation kit (Ambion) and purified on M2-agarose (Sigma). Varying concentrations of VEGFR2-Fc (0–200 nM) or VEGFR1-Fc (1–100 nM) were incubated with a constant concentration of the purified binder protein (0.2 or 0.5 nM) at 30ºC for 30 min in buffer C (1× PBS, 0.02% Triton X-100 [pH 7.4]). The receptor-binder complexes were captured by using Protein A magnetic beads for 10 min at room temperature on a Kingfisher. The beads were washed six times with 100 μl buffer C, and the protein was eluted with 100 μl 0.1 M KOH. Samples were dried onto a LumaPlate-96 (Packard), and the amount of ^{35}S on the plate was measured with a TopCount NXT instrument (Packard). Data were analyzed by using the GraphPad Prizm software (GraphPad Software, Inc., San Diego, CA), fitted with a one-site, nonlinear binding equation.

Expression and Purification of Binder Proteins in *E. coli*

Binder proteins were expressed by using a pET9d vector in *E. coli* BL21 (DE3) pLysS cells (Invitrogen). After induction and expression, cell pellets were collected and resuspended in 50 ml lysis buffer D (50 mM NaH_2PO_4 [pH 8.0], 0.5 M NaCl, 5% glycerol, 5 mM CHAPS, 25 mM imidazole, 1× Complete Protease Inhibitor Cocktail [Roche]) and sonicated on ice. The soluble fraction was separated by centrifugation, and the supernatant was rotated for 1 hr at 4ºC with 10 ml TALON Superflow Metal Affinity Resin (Clontech) preequilibrated with buffer E (50 mM NaH_2PO_4, 0.5 M NaCl, 5% glycerol, 25 mM imidazole [pH 8.0]). The resin was washed with 10 column volumes of buffer E and 30 column volumes of buffer F (1× PBS [pH 7.4], 25 mM imidazole [pH 7.4]). Protein was eluted with 1× PBS, 250 mM imidazole (pH 7.4) and was dialyzed against 1× PBS at 4ºC.

BIAcore Analysis

Using a BIAcore 2000, human and mouse VEGFR2-Fc were immobilized onto a CM5 sensor chip, and binding proteins (0–100 nM) were injected in buffer G (10 mM HEPES, 150 mM NaCl, 0.005% Tween 20 [pH 7.4]). Rate constants, *kon* and *koff*, and the affinity constant, K_d, were calculated by using BIA Evaluation 2.0 (BIAcore).

For inhibition experiments, human $VEGF_{165}$ was immobilized on a CM5 chip, and KDR-Fc (20 nM) was injected in the presence of binding proteins (0–100 nM). IC_{50} represented the binder concentration at which 50% reduction of KDR binding to VEGF was observed.

Construction of Stable Cell Lines

DNA encoding chimeric receptors composed of the transmembrane and cytoplasmic domains of the human erythropoietin receptor (EpoR, amino acids 251–508) fused to the extracellular domains of KDR (amino acids 1–764), Flk-1 (amino acids 1–762), or human TrkB receptor (amino acids 1–430) were constructed by overlapping PCR and were cloned into the EcoRI and XhoI sites of pcDNA 3.1(+) (Invitrogen) to generate the plasmids phKE8 (KDR/EpoR fusion), pmKE2 (Flk-1/EpoR fusion), and phTE (TrkB/EpoR fusion).

Construction of Cell Lines for Flow Cytometry

CHO-K1 cells (ATCC, Manassas, VA) were stably transfected by using Lipofectamine 2000 (Invitrogen) with either pcDNA 3.1

(Invitrogen), pmKE2, or a mixture of pcDNA 3.1 and a plasmid encoding full-length human KDR (Origene Inc., clone PR1371-H11). Stable transfectants were selected and maintained in the presence of 0.5 mg/ml Geneticin (Invitrogen). The human KDR-expressing clone (CHO-KDR) and the murine Flk-1/EpoR chimera-expressing population (CHO-Flk-1) were obtained by fluorescence-activated cell sorting of the transfected population after staining with an anti-KDR polyclonal antiserum (R&D Systems). CHO-KDR and CHO-Flk-1 cell lines were grown routinely in Dulbecco's modified Eagle's medium (DMEM; GIBCO-BRL) supplemented with 10% (v/v) fetal bovine serum (FBS), 0.5 mg/ml Geneticin, 100 U/ml penicillin, 0.25 μg/ml amphotericin B, 100 μg/ml streptomycin, and 2 mM L-glutamine.

Construction of Ba/F3 Cell Lines

Cell lines that would proliferate in response to VEGF were constructed by transfection of the murine pre-B cell line Ba/F3 (DSMZ, Braunschweig, Germany) with phKE8, pmKE2, and phTE. Ba/F3 cells were maintained in minimal Ba/F3 medium (RPMI-1640, GIBCO-BRL) containing 10% FBS, 100 U/ml penicillin, 0.25 μg/ml amphotericin B, 100 μg/ml streptomycin, and 2 mM L-glutamine supplemented with 10% conditioned medium from WEHI-3B cells (DSMZ; grown in Iscove's modified Dulbecco's medium [GIBCO-BRL]/10% FBS/25 μM β-mercaptoethanol) as a source of essential growth factors. After electroporation, stable transfectants were selected in 0.75 mg/ml Geneticin and were maintained in the presence of 100 ng/ml human $VEGF_{165}$ (Ba/F3-KDR and Ba/F3-Flk-1 populations) or human NT4 (Ba/F3-TrkB).

Cell Surface Binding

Cell surface KDR and Flk-1 binding was analyzed simultaneously on VEGFR2-expressing and control cells by flow cytometry. CHO-pcDNA3 cells (control) were released from their dishes with trypsin-EDTA, washed in Dulbecco's PBS without calcium and magnesium (D-PBS^-; Invitrogen), and stained for 30 min at 37ºC with 1.5 μM CMTMR (5-(and-6)-(4-chloromethyl)benzoyl)amino)-tetramethylrhodamine) (Molecular Probes). The cells were washed in D-PBS^-, incubated for an additional 30 min at 37ºC, and then resuspended in blocking buffer (D-PBS^-/10% fetal bovine serum) on ice. CHO-KDR or CHO-Flk-1 cells were treated identically, except that CMTMR was omitted. A total of 75,000 of CMTMR-stained CHO-pcDNA3 cells were mixed with an equal number of unstained CHO-KDR or CHO-Flk-1 cells in each well of a V-bottom 96-well plate. All antibodies and binding proteins were diluted in 25 μl/well blocking buffer, and each treatment was conducted for 1 hr at 4ºC. Cell mixtures were stained with His_6-tagged binding proteins, washed twice with cold D-PBS^-, and then treated with 2.5 μg/ml anti-His_6 MAb (R&D Systems), washed, and stained with 4 μg/ml Alexa Fluor 488-conjugated anti-mouse antibody (Molecular Probes). For cells treated with an anti-KDR mouse monoclonal antibody (Accurate Chemical, Westbury, NY) or an anti-Flk-1 goat polyclonal antibody (R&D Systems), the anti-His_6 step was omitted, and antibody binding was detected with the species-appropriate Alexa Fluor 488-conjugated secondary antibody (Molecular Probes). After staining, cells were resuspended in 200 μl/well D-PBS^-/1% FBS/1 μg/ml 7-aminoactinomycin D (7-AAD; Molecular Probes) and analyzed by flow cytometry on a FACSCalibur (Becton Dickinson, San Jose, CA) equipped with a 488 nM laser. After gating to exclude dead cells (7-AAD-positive), VEGFR2-expressing cells and CHO-pcDNA3 cells were measured independently for Alexa Fluor 488 fluorescence by gating on the CMTMR-negative or -positive populations, respectively. Control experiments showed that staining with CMTMR did not interfere with the detection of Alexa Fluor 488-conjugated antibodies on the surface of the stained cells (data not shown).

Cell surface binding was also assessed by fluorescence microscopy with the secondary antibodies described above. For these studies, antibodies were diluted in D-PBS containing calcium and magnesium (D-PBS^+)/10% FBS. Cells were grown on 24- or 96-well plates, and, after staining, they were kept in D-PBS^+ for observation on an inverted fluorescence microscope.

Cell Proliferation Assay

Ba/F3 cells were washed three times in minimal Ba/F3 medium and were resuspended in the same medium containing 15.8 ng/ml human $VEGF_{165}$, mouse $VEGF_{164}$, or hNT4, and 95 μl containing 5×10^4 Ba/F3-KDR, 2×10^4 Ba/F3-Flk-1, or Ba/F3-TrkB cells, respectively, were added per well to a 96-well tissue culture plate. A total of 5 μl serial dilutions of test protein in PBS/20% minimal Ba/F3 medium was added to each well. After incubation for 72 hr at 37ºC, proliferation was measured by the addition of 20 μl CellTiter 96 AQueous One Solution Reagent (Promega) to each well, incubation for 4 hr at 37ºC, and measurement of the absorbance at 490 nm with a microtiter plate reader (Molecular Dynamics).

HUVEC cells (Human Umbilical Vein Endothelial Cells, Clonetics, Walkersville, MD) from passages 2–6 were grown in EGM-2 medium (Clonetics). A total of 5000 cells/well were resuspended in 200 μl starvation medium (equal volumes of DMEM [GIBCO-BRL] and F-12K medium [ATCC]), supplemented with 0.2% fetal bovine serum and 1× penicillin/streptomycin/fungizone solution (GIBCO-BRL), plated in 96-well tissue culture plates, and incubated for 48 hr. Binding proteins were added to the wells and incubated for 1 hr at 37º, and then human $VEGF_{165}$ was added to a final concentration of 16 ng/ml. After 48 hr, cell proliferation was measured by the addition of 30 μl to each well of a mixture of 1.9 mg/ml CellTiter96 AQueous MTS reagent (Promega) with 44 μg/ml phenazine methosulfate (Sigma) and measurement of absorbance at 490 nm as described above for Ba/F3 cells.

Acknowledgments

We are grateful to Dr. Edward Fritsch for his insightful suggestions and discussions on the manuscript as well as the experimental part of the work. We are also thankful to Dr. Brian Seed and Dr. Jack Szostak for helpful comments on the manuscript.

Received: September 1, 2005
Revised: November 16, 2005
Accepted: December 27, 2005
Published: May 29, 2006

References

1. Amstutz, P., Forrer, P., Zahnd, C., and Plückthun, A. (2001). *In vitro* display technologies: novel developments and applications. Curr. Opin. Biotechnol. *12*, 400–405.
2. Lipovsek, D., and Plückthun, A. (2004). In-vitro protein evolution by ribosome display and mRNA display. J. Immunol. Methods *290*, 51–67.
3. Takahashi, T.T., Austin, R.J., and Roberts, R.W. (2003). mRNA display: ligand discovery, interaction analysis and beyond. Trends Biochem. Sci. *28*, 159–165.
4. Nygren, P.A., and Skerra, A. (2004). Binding proteins from alternative scaffolds. J. Immunol. Methods *290*, 3–28.
5. Koide, A., Bailey, C.W., Huang, X., and Koide, S. (1998). The fibronectin type III domain as a scaffold for novel binding proteins. J. Mol. Biol. *284*, 1141–1151.
6. Xu, L., Aha, P., Gu, K., Kuimelis, R.G., Kurz, M., Lam, T., Lim, A.C., Liu, H., Lohse, P.A., Sun, L., et al. (2002). Directed evolution of high-affinity antibody mimics using mRNA display. Chem. Biol. *9*, 933–942.
7. Koide, A., Abbatiello, S., Rothgery, L., and Koide, S. (2002). Probing protein conformational changes in living cells by using designer binding proteins: application to the estrogen receptor. Proc. Natl. Acad. Sci. USA *99*, 1253–1258.
8. Karatan, E., Merguerian, M., Han, Z., Scholle, M.D., Koide, S., and Kay, B.K. (2004). Molecular recognition properties of FN3 monobodies that bind the Src SH3 domain. Chem. Biol. *11*, 835–844.
9. Ferrara, N. (2004). Vascular endothelial growth factor: basic science and clinical progress. Endocr. Rev. *25*, 581–611.
10. Shibuya, M. (2003). Vascular endothelial growth factor receptor-2: its unique signaling and specific ligand, VEGF-E. Cancer Sci. *94*, 751–756.
11. Folkman, J. (2004). Endogenous angiogenesis inhibitors. APMIS *112*, 496–507.
12. Huang, J., Frischer, J.S., Serur, A., Kadenhe, A., Yokoi, A., McCrudden, K.W., New, T., O'Toole, K., Zabski, S., Rudge, J.S., et al. (2003). Regression of established tumors and

metastases by potent vascular endothelial growth factor blockade. Proc. Natl. Acad. Sci. USA *100*, 7785–7790.

13. Eskens, F.A. (2004). Angiogenesis inhibitors in clinical development; where are we now and where are we going? Br. J. Cancer *90*, 1–7.
14. Midgley, R., and Kerr, D. (2005). Bevacizumab–current status and future directions. Ann. Oncol. *16*, 999–1004.
15. Roberts, R.W., and Szostak, J.W. (1997). RNA-peptide fusions for the in vitro selection of peptides and proteins. Proc. Natl. Acad. Sci. USA *94*, 12297–12302.
16. Nemoto, N., Miyamoto-Sato, E., Husimi, Y., and Yanagawa, H. (1997). In vitro virus: bonding of mRNA bearing puromycin at the 3′-terminal end to the C-terminal end of its encoded protein on the ribosome in vitro. FEBS Lett. *414*, 405–408.
17. Ferrara, N., and Davis-Smyth, T. (1997). The biology of vascular endothelial growth factor. Endocr. Rev. *18*, 24–25.
18. Main, A.L., Harvey, T.S., Baron, M., Boyd, J., and Campbell, I.D. (1992). The three-dimensional structure of the tenth type III module of fibronectin: an insight into RGD-mediated interactions. Cell *71*, 671–678.
19. Claffey, K.P., Wilkison, W.O., and Spiegelman, B.M. (1992). Vascular endothelial growth factor. Regulation by cell differentiation and activated second messenger pathways. J. Biol. Chem. *267*, 16317–16322.
20. Shima, D.T., Kuroki, M., Deutsch, U., Ng, Y.S., Adamis, A.P., and D'Amore, P.A. (1996). The mouse gene for vascular endothelial growth factor. Genomic structure, definition of the transcriptional unit, and characterization of transcriptional and post-transcriptional regulatory sequences. J. Biol. Chem. *271*, 3877–3883.
21. Lee, J., Gray, A., Yuan, J., Luoh, S., Avraham, H., and Wood, W.I. (1996). Vascular endothelial growth factor-related protein: a ligand and specific activator of the tyrosine kinase receptor Flt4. Proc. Natl. Acad. Sci. USA *93*, 1988–1992.
22. Parker, M.H., Chen, Y., Danehy, F., Dufu, K., Ekstrom, J., Getmanova, E., Gokemeijer, J., Xu, L., and Lipovsek, D. (2005). Antibody mimics based on human fibronectin type three domain engineered for thermostability and high-affinity binding to vascular endothelial growth factor receptor two. Protein Eng. Des. Sel. *18*, 435–444.
23. Lu, D., Shen, J., Vil, M.D., Haifan Zhang, H., Jimenez, X., Bohlen, P., Witte, L., and Zhu, Z. (2003). Tailoring in vitro selection for a picomolar affinity human antibody directed against vascular endothelial growth factor receptor 2 for enhanced neutralizing activity. J. Biol. Chem. *278*, 43496–43507.
24. Vartanian, J.P., Henry, M., and Wain-Hobson, S. (1996). Hypermutagenic PCR involving all four transitions and a sizeable proportion of transversions. Nucleic Acids Res. *24*, 2627–2631.
25. Kurz, M., Gu, K., and Lohse, P.A. (2000). Psoralen photo-crosslinked mRNA-puromycin conjugates: a novel template for the rapid and facile preparation of mRNA-protein fusions. Nucleic Acids Res. *28*, E83.